VDMA
Fluid Power Association

22nd ISC

International Sealing Conference

Stuttgart, Germany
October 01 - 02, 2024

Sealing Technology –
Challenges accepted!

UNI STUTTGART

ISBN 978-3-8163-0768-6

Fachverband Fluidtechnik im VDMA e. V. Lyoner Str. 18
50628 Frankfurt am Main
Germany

Phone +49 69 6603-1513
E-Mail maximilian.baxmann@vdma.org
Internet www.vdma.org/fluid

Enabling more sustainable sealing solutions via multi-scale friction modelling

Dr. Meghshyam Shisode, Dr. Ron Willems, Dr. Bas van der Vorst, Dr. Mickael Sansalone

A reliable and accurate seal friction model is paramount in optimizing sealing products towards energy-efficient and sustainable sealing systems. In seals, depending on the contact conditions, boundary and mixed lubrication regimes are as prevalent as the full-film regime due to, for example, counterface roughness, lubricant starvation, low speed, severe contact pressure, temperature, etc. Although the research on full-film lubrication regime is well matured, a reliable predictive model for rubber dry friction, contributing to boundary and mixed lubrication regimes, is still lacking, therefore hindering the friction and wear models accuracy for sealing applications.

In this work, a predictive analytical model to estimate temperature and speed dependent rubber dry friction is proposed. The model is inspired by a multi-scale representation of a metallic counterface combined with a first-order analytical approximation of contact stresses and rubber deformation. The counterface is decomposed into different scales of roughness and the rubber dissipation energy is then determined on each scale. The transition between different scales is also modeled, which is important to correctly estimate the contribution from each scale. Subsequently, a cumulative frictional energy loss is estimated to predict the friction force.

The resulting model is able to predict temperature and sliding speed dependent friction coefficient and shows a good correlation with in-house experiments. The proposed dry friction model can be combined with the lubricant viscous shearing friction model to predict the overall friction more reliably in the sealing contact, thereby accelerating the design of more sustainable and energy-efficient sealing solutions.

1 Introduction

Currently, there is significant momentum in both the industrial and automotive sectors to reduce seal friction while simultaneously enhancing seal wear resistance and longevity. One of the key customer requirements is to minimize the rotating shaft seal friction torque, which improves system efficiency, reduces energy consumption, and lowers overall carbon emissions. Given stricter CO_2 regulations, the challenge lies in designing optimal sealing solutions with reduced friction. To address this, new predictive tools are being developed to estimate seal friction, thereby streamlining the testing process and accelerating time to market.

In sealing contacts, total friction arises from two main sources: material friction due to direct asperity contact and friction resulting from lubricant viscous shearing. The specific contributions of material friction and lubricant viscous shearing depend on various factors such as material properties, speed, surface topography, contact load, counterface wetting and temperature. While models have matured significantly in estimating friction due to lubricant viscous shearing, research is still evolving regarding the modeling of rubber material friction resulting from direct asperity contact. The objective of our research initiative is hence to develop a physics-based, simplified and reliable approach for predicting rubber dry friction in sealing applications, with the aim to provide rapid solutions for end-users.

Rubber dry friction is a complex phenomenon fundamentally related to the viscoelastic nature of the material. In dry conditions, the interface conditions become significant, as adhesion effects are generally activated and may contribute to viscoelastic friction. Under lubricated conditions, the effect of adhesion is expected to substantially reduce due to the presence of a lubricant layer that inhibits direct intermolecular bonding between the rubber and metal counterface. However, viscoelastic friction still predominantly exists in boundary and mixed lubrication regimes. Therefore, this study focuses on modeling the viscoelastic friction, in alignment with its relevance for sealing applications.

Grosch [1] conducted the first experimental study on dry friction in rubber. In this research, rubber pads were slid across glass, steel, and abrasive plates, resulting in viscoelastic deformation within the rubber material. The study revealed that rubber friction reached a maximum at a specific speed, declining at higher speeds. Interestingly, the speed at which this maximum friction occurred shifts with temperature as described by the Williams–Landel–Ferry (WLF) equation [2]. This equation is based on measurements of rubber viscoelastic properties. Grosch's observations led to the conclusion that near-surface viscoelastic deformation plays a crucial role in dry rubber friction.

In the literature, two main theories of rubber dry friction have been published. One theory, proposed by Klüppel and Heinrich [3], and another by Persson [4], both focus heavily on the multi-scale nature of counterface and their fractal roughness. Persson et al. [4] developed condensed but mathematically complex equations to predict rubber friction. However, these models rely on strong assumption of truncating the fractal surface spectrum to a chosen wavevector (q_1), which makes them less robust as the viscoelastic loss significantly depends on the choice of truncation wavevector (q_1).

In 2000, Wassink et al. [5] proposed a physical model for seal viscoelastic friction. Wassink used a multi-scale description of surface roughness. They decomposed the counterface into 16 different scales. When a seal slides over a rough shaft, the seal material must deform to move past the asperities on the shaft surface. Since the seal material is viscoelastic, the deformation and recovery processes result in energy loss, contributing to total friction. By determining the energy loss per roughness scale, the overall viscoelastic friction is estimated. The results from Wassink's model show a good qualitative correlation with experimental data. However, the model requires specification of multiple fitting parameters, which limits its versatility.

This paper proposes a different approach to address the challenges encountered with existing models. Rather than considering a continuous spectrum of frequencies used in [3] [4], a discrete set of scales is proposed to describe the counterface topography. This model is based on the concept of determining energy loss due to viscoelastic material behavior of rubber interacting at various roughness scales on the contacting metallic surface, similar to the approach described by Wassink et al. [5]. However, unlike the Wassink model, the model proposed in this paper requires only a single model parameter.

2 Multi-scale dry friction model

This section introduces a first-order model for rubber friction. The model is built upon a multi-scale representation of the counterface and utilizes analytical equations to calculate stresses and deformations in rubber. The predictions highlight the significance of multi-scale surface roughness effects and their relationship with rubber material properties in dry friction. Key parameters governing rubber friction include contact temperature and speed. For example, the coefficient of friction can vary between 0.1 and 2, depending on the speed and temperature combination.

2.1 Multi-scale decomposition of surface roughness

While standard steel-to-steel friction models employ a single-scale representation of surface roughness, predicting rubber friction necessitates a multi-scale description of the counterface. In fact, such an approach is required to account for all dissipative phenomena generated during sliding. The method proposed in this paper considers a discrete number of scales. For simplicity, each scale is represented as a sinusoidal function. Moreover, to avoid superposition of dissipative effects, these scales must be distinct from each other. Consequently, a maximum of five scales is utilized in the proposed approach to cover the frequency range developed onto the surface. The counterface is first measured using confocal microscopy, and 2D profiles in the sliding direction are extracted. By discretizing each profile using Fourier transform and then applying inverse Fourier transform, five distinct roughness scales are determined for each of the original 2D profiles. For each scale of 2D profile obtained, parameters such as roughness R_a, wavelength λ, and mean asperity radius R (Equation (1)) can be determined. Figure 1 illustrates the example of a measured 2D profile and its corresponding five different roughness scales, while Table *1* provides details of roughness parameters for each scale.

$$R = \frac{\lambda^2}{2\pi R_a} \tag{1}$$

Table 1: Roughness parameters for different scales

Scale	1	2	3	4	5
Wavenumber domain (m^{-1})	<11359	11359 - 31552	31552 - 88346	88346 - 239797	239797 - 646190
Ra (um)	0.15	0.10	0.06	0.05	0.03
Wavelength (um)	162.5	29.7	11.5	4.9	2.2

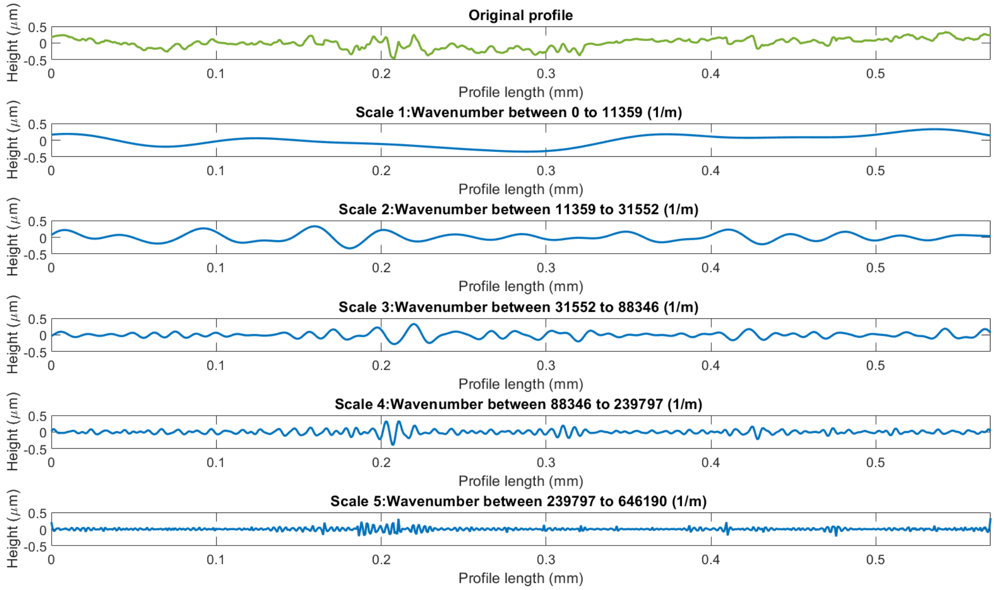

Figure 1: Measured profile of a counterface ($R_a = 0.45\mu m$) and its decomposition into 5 roughness scales

2.2 Dry friction model for viscoelastic dissipation

A simple analytical model is proposed to predict the friction resulting from the bulk deformation of rubber at each discretized scale of the counterface. The model assumes that the deformation and release of rubber at each scale lead to energy dissipation due to its viscoelastic nature. The resulting friction is derived by summing up all the dissipative effects generated at different scales. Additionally, the model assumes that only the rubber surface deforms, while the metallic counterface asperities remain rigid. When metallic asperities slide on a rubber surface, the total strain energy due to bulk rubber deformation can be expressed as follows:

$$\Delta E_T = \iint_{Volume,time} \sigma_{ij} \frac{d\varepsilon_{ij}}{dt} dt dV \tag{2}$$

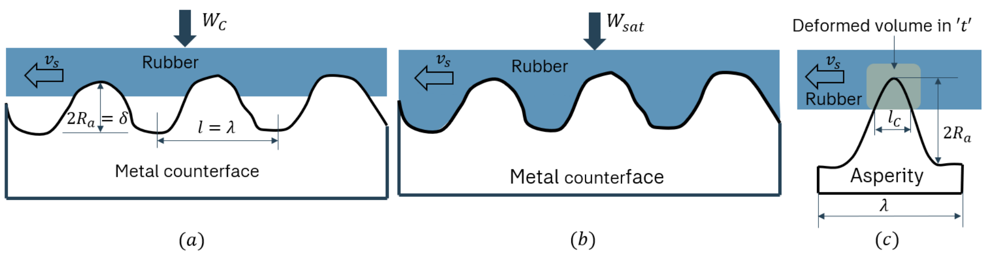

Figure 2: Sliding of rubber on metal counterface (a) in unsaturated contact condition (b) in saturated contact condition (c) single asperity contact

where σ_{ij} and ε_{ij} are the stress and strain components respectively. Since the roughness scale of the metallic counterface is described as a sinusoidal function, stresses and deformations are also assumed to respond in the same manner in time and space. This allows for the energy dissipation to be approximated as:

$$\Delta E = -\varepsilon_C \sigma_C \frac{G"(\omega_C)}{G^*(\omega_C)} V_{def} \tag{3}$$

where V_{def} is the considered deformed volume of rubber (Figure 2c) and ω_C the frequency of deformation. G^* is the combined shear modulus and $G"$ is the loss shear modulus. Considering v_s to be the sliding speed and l_C, the contact length at asperity in the sliding direction, the frequency ω at which rubber is excited at this scale, and the deformed volume during time t, can be expressed as:

$$\omega = \frac{v_s}{\lambda}, \qquad V_{def} = S_{def}\, v_s t \tag{4}$$

where S_{def} is the deformed section in the plane perpendicular to the sliding direction. Finally, assuming the behavior of rubber to be linear elastic, the energy dissipated can be written as:

$$\Delta E \approx -G"(\omega_C) \frac{\sigma_C^2}{3G^*(\omega_C)^2} S_{def} v_s t \tag{5}$$

The total dissipated energy and the frictional force F_{fric} can be calculated as follows:

$$\Delta E \approx \sum_{i=1}^{n_{scale}} -n_{a_i} G"(\omega_i) \frac{\sigma_i^2}{3G^*(\omega_i)^2} S_{def,i} v_s t \tag{6}$$

$$F_{fric} \approx k_f \sum_{i=1}^{n_{scale}} n_{a_i} G"(\omega_i) \frac{\sigma_i^2}{3G^*(\omega_i)^2} S_{def,i} \tag{7}$$

where n_{a_i} is the number of asperities at scale i and k_f is the model parameter determined by reducing the error in model results and experiments. The parameter k_f is introduced to account for complex phenomena that are not adequately captured by the proposed first-order model. The coefficient of friction resulting from viscoelastic losses is then estimated as follows:

$$\mu_{dry} = \frac{F_{fric}}{W_C} = \frac{F_{fric}}{A_C P_C} \tag{8}$$

where W_C, P_C and A_C are normal contact load, mean contact pressure and apparent contact area respectively. Finally, the coefficient of friction estimated for each 2D profile is averaged to determine the overall dry friction coefficient.

2.2.1 Geometry and stresses for a single asperity

The asperity level calculations of stress and deformations are based on the Hertzian theory and on Johnson developments [6] for elastic contacts of sinusoidal surfaces. The number of asperities n_{a_i} and load on each asperity W_i at scale i can be determined as:

$$n_{a_i} = \frac{A_C}{\lambda_i^2}, \quad W_i = \frac{W_C}{n_{a_i}} \tag{9}$$

According to the Hertzian theory, the contact area is defined by the following diameter of contact l_i:

$$l_i = 2\left(\frac{3}{16}\frac{W_i R_i}{G^*(\omega_i)}\right)^{1/3} \tag{10}$$

where R_i is the mean radius of asperity (Equation (1)) and ω_i is the frequency at scale i (Equation (4)). The mean contact stress can thus be expressed as:

$$\sigma_i = \frac{4W_i}{\pi l_i^2} \tag{11}$$

These equations are valid when the penetration of an asperity into the rubber is relatively small. However, as the load increases, saturation occurs, and the rubber fully penetrates the contacting surface asperities (see Figure 2b). Under such situation a different equation is required. Johnson [6] showed that the stress at which saturation occurs can be calculated as:

$$\sigma_{sat,i} = \frac{8\pi R_{a_i} G^*(\omega_i)}{\lambda_i} \tag{12}$$

When the saturation stress ($\sigma_{sat,i}$) is reached, $\sigma_i = \sigma_{sat,i} = P_C$, $l_i = \lambda_i$, $\delta_i = 2R_{a_i}$ and since the stress varies between 0 and $\sigma_{sat,i}$, a following relation is assumed between contact stress σ_i and penetration depth δ_i:

$$\delta_i = 4R_{a_i}\left(\frac{\sigma_i}{\sigma_i + \sigma_{sat,i}}\right) \tag{13}$$

From these relations, the deformed section of rubber can be estimated as:

$$S_{def,i} = l_i \delta_i \tag{14}$$

Finally using Equation (7), the friction force at each asperity scale can be calculated.

2.2.2 Roughness scale interaction

Up until now, dissipative effects have been estimated independently at each scale and then aggregated to determine the overall frictional energy loss. However, this approach ignores the interaction and effects of roughness scale at subsequent scales. An important parameter influenced by scale interaction is indeed the apparent area available at the subsequent scale.

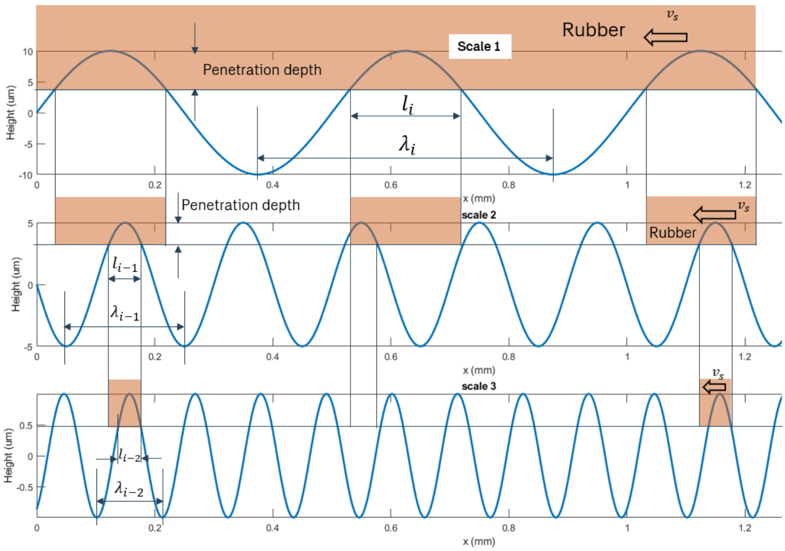

Figure 3: Illustration of subsequent roughness scales interaction

As illustrated in Figure 3, if the apparent area available at scale i is A_C then at scale $(i+1)$, the total available apparent contact is $A_{corrected} = A_{f_{i+1}} * A_C = \frac{l_i}{\lambda_i} A_C$ where $A_{f_{i+1}}$ is the area correction factor. Similarly, for scale $(i+2)$, $A_{corrected} = A_{f_{i+2}} * A_C = \frac{l_{i-1}}{\lambda_{i-1}} * \frac{l_i}{\lambda_i} A_C$. Therefore, at scale $i = 1, A_{corrected} = A_C$ and for all subsequent scales $i > 1, A_{corrected} = A_{f_i} * A_C$. Accordingly, the number of asperities n_{a_i} and load on asperity W_i (Equation (9)) at scale i are updated to account for the roughness scale interaction.

2.2.3 Viscoelastic friction computation

The detailed flow used to compute the viscoelastic dry rubber friction can then be described as illustrated in Figure 4 below:

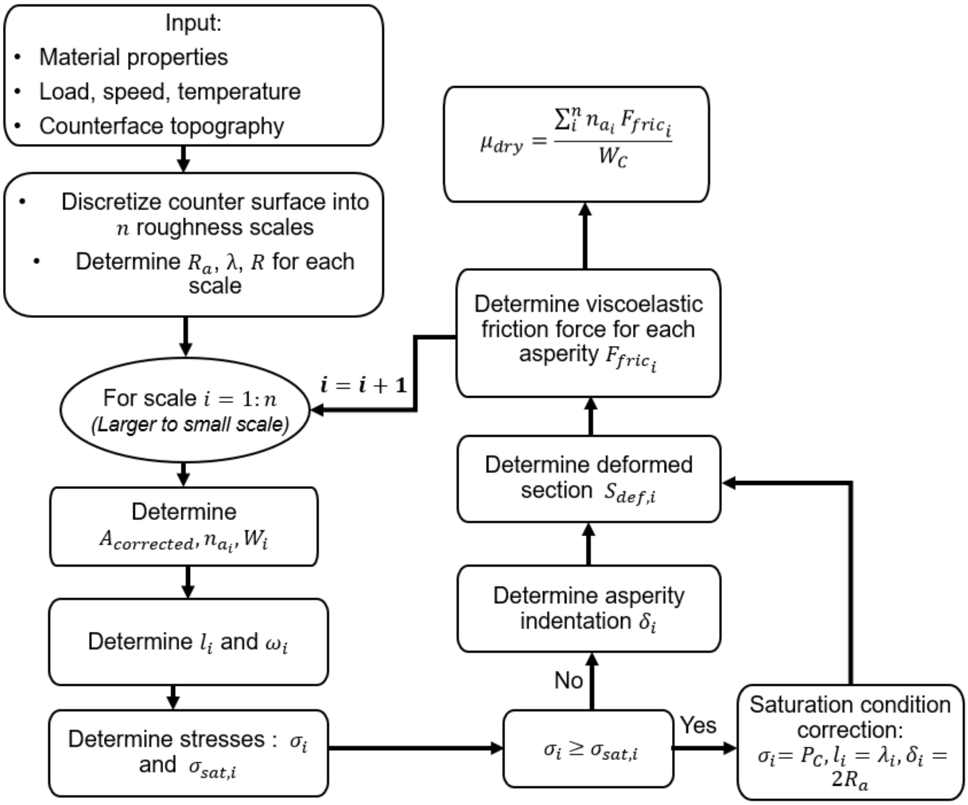

Figure 4: Flow chart: rubber viscoelastic friction computation in dry contact condition

3 Experiments and model validation

Rubber friction highly depends on the operational conditions. Under dry conditions, the coefficient of friction can vary between 0.1 and 2, depending on the speed and temperature. Therefore, it is necessary to characterize rubber friction across various temperatures and sliding speeds. To achieve this, an in-house CETR universal tribometer is used to measure the dry friction coefficient using a rubber ring on a steel disk configuration and across a range of relevant temperatures and sliding speeds.

3.1 Tribometer set-up and friction measurement

The setup principle is illustrated in Figure 5. A stationary ring made of elastomer material, applies load against a rotating steel disk. A 3D load sensor measures the resulting frictional torque. The ring, along with its support and the load sensor, can be vertically displaced to load and unload the sample. To ensure alignment between the ring and disk surfaces, the ring is mounted on a ball joint. The tribometer features an insulated chamber, allowing tests at temperatures ranging from -20°C to +150°C under stable conditions. The ring's inner diameter is 32mm, and the outer diameter is 40mm. An electrical motor drives the steel disk at a predefined rotational speed. To minimize self-heating during contact, the maximum rotational speed range is limited to 0.01 to 50 RPM, which corresponds to a linear sliding speed range of 0.02 to 95mm/s. Experiments are conducted at different temperatures (25°C to 85°C) and with a normal load, resulting in a nominal contact pressure of 0.1 - 0.2 MPa. For a given temperature and normal load, speed sweeps from 0.02 to 95 mm/s are repeated at least twice. The coefficient of friction is then determined based on the stable part of the friction torque curve obtained for each speed. Ultimately, the average coefficient of friction is calculated across repetitions for a specific speed, temperature, and normal load combination.

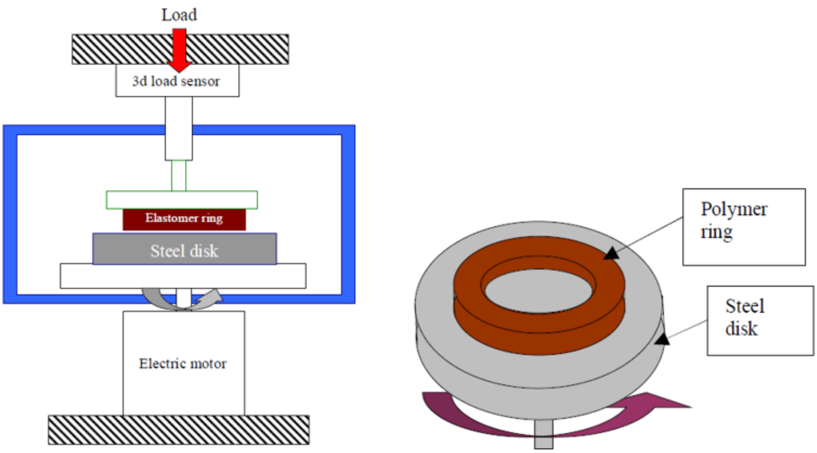

Figure 5: Tribometer setup

3.2 Samples

Several proprietary fluoro-elastomers (FKM1, FKM2, FKM3 and FKM4) are used for this study. The required material properties are thus procured from a proprietary sealing material' database. The counterface used is a steel disk of 54mm diameter and a surface roughness of $R_a = 0.5\mu m$. The surface is purposefully plunge ground resulting in a roughness pattern oriented in the sliding (circumferential) direction, as shown in Figure 6.

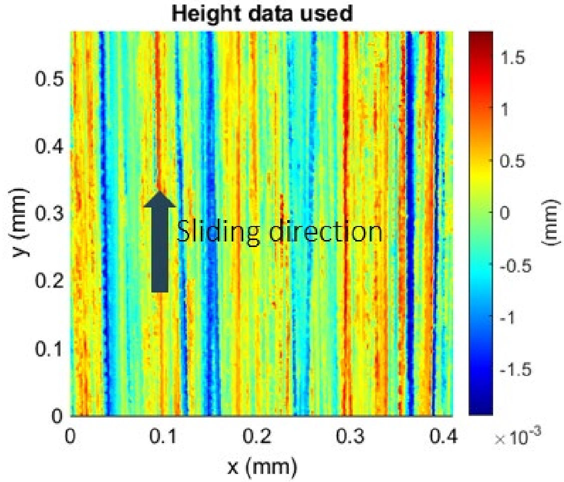

Figure 6: Surface topography of steel counterface

3.3 Results: model vs. experiments

The experimental results and their comparison with the model for four different FKM materials are shown in Figure 7 to 10. It should be noted that, the unique model parameter k_f is derived by minimizing the difference between experiments and the model prediction for FKM1, FKM2, and FKM3 materials. Subsequently, this derived parameter is applied to validate the model for FKM4 material. The comparison reveals a strong qualitative and quantitative correlation between the model predictions and experimental data across the whole range of speed and temperature considered.

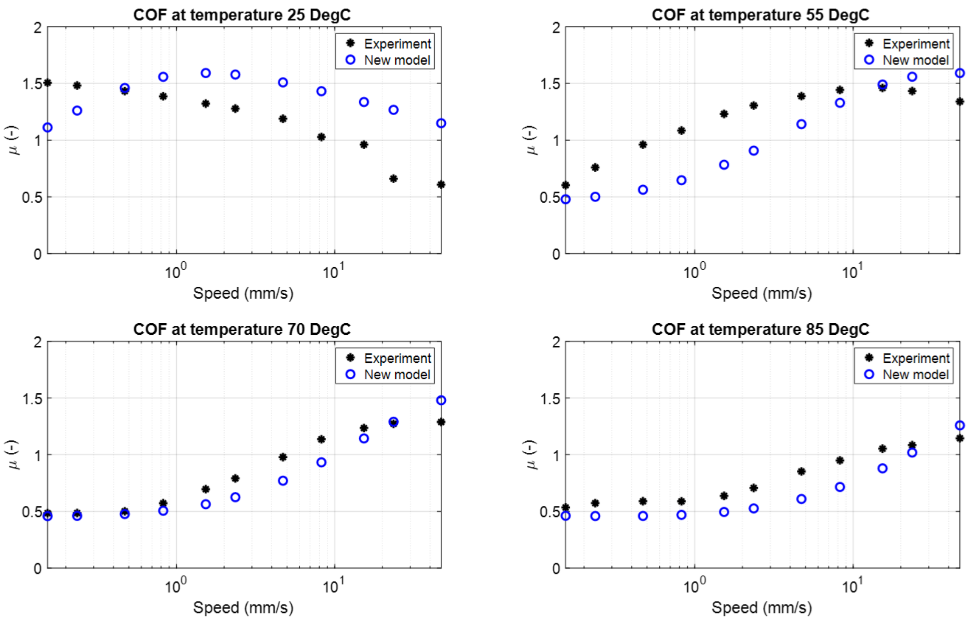

Figure 7: Coefficient of friction (COF) comparison for FKM1; model vs. experiments

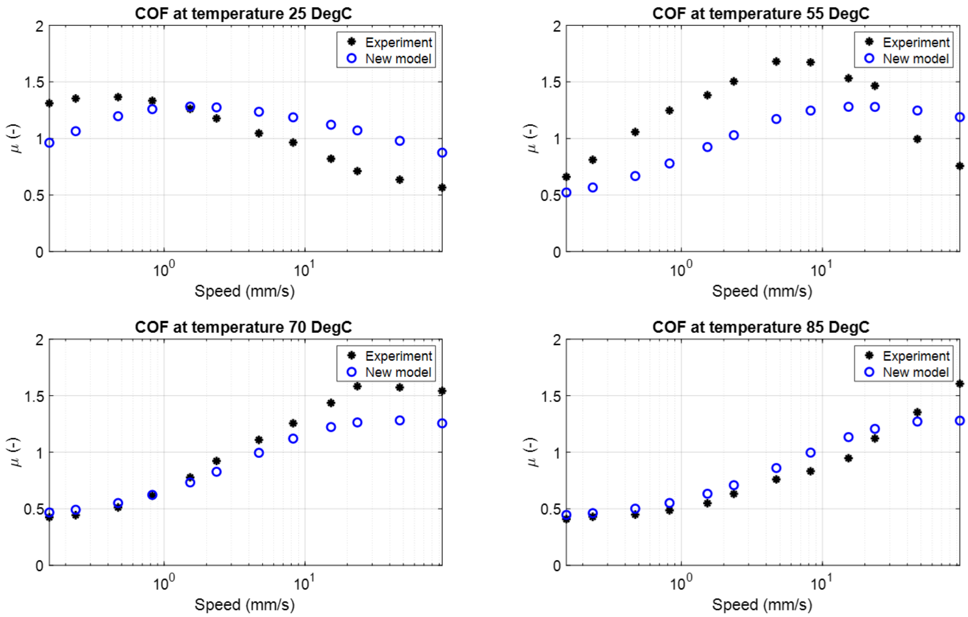

Figure 8: Coefficient of friction (COF) comparison for FKM2; model vs. experiments

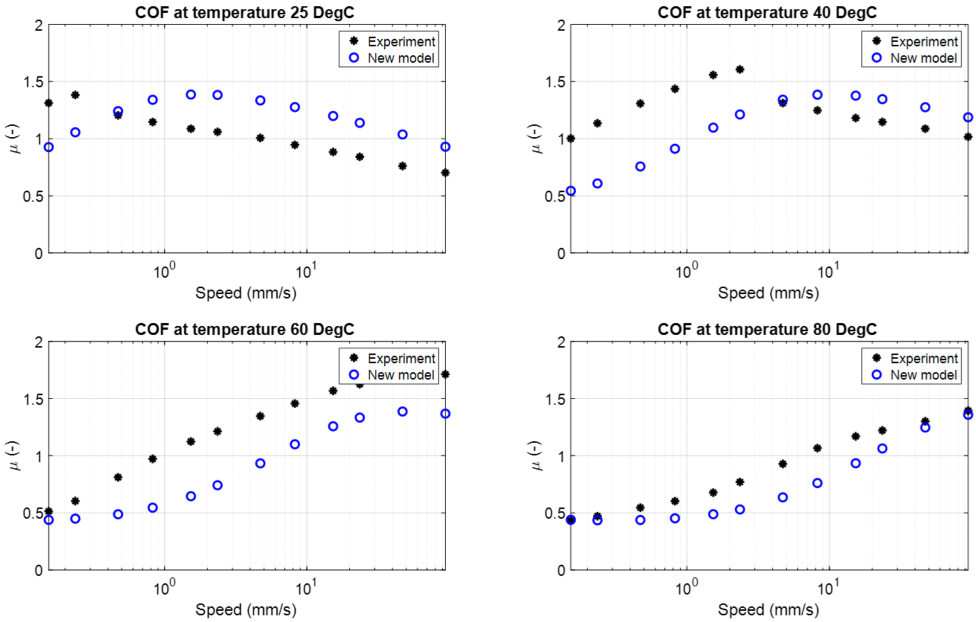

Figure 9: Coefficient of friction (COF) comparison for FKM3; model vs. experiments

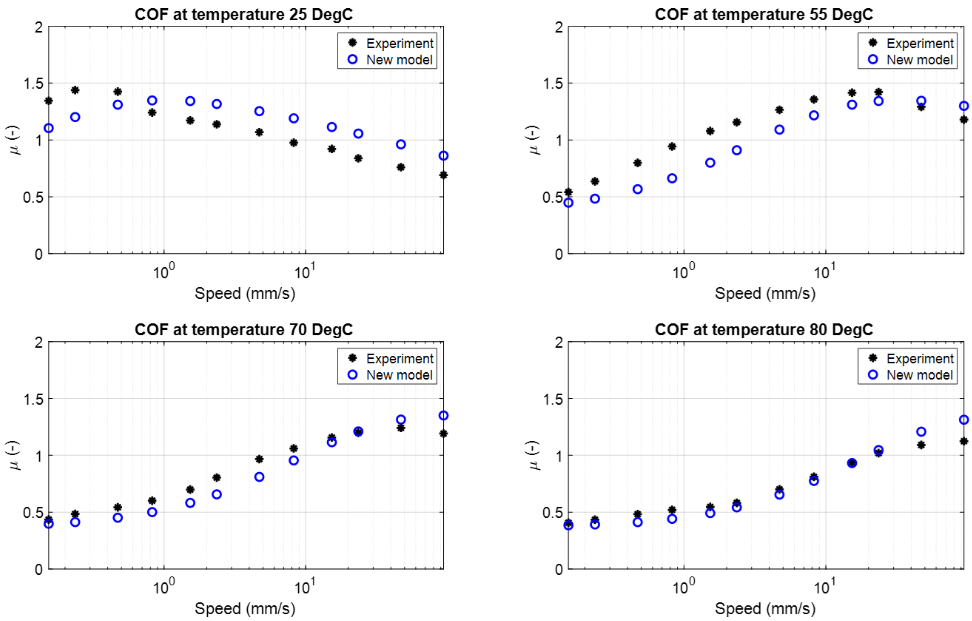

Figure 10: Coefficient of friction (COF) comparison for FKM4; model vs. experiments

4 Seal material optimization for sustainability

The urgent need to address climate change has led to a growing focus on sustainability. It is crucial to engage all stakeholders across the entire value chain, including suppliers, manufacturers, and customers, in discussions about the environmental impact of our products. As part of SKF's commitment to sustainability, web-based calculation tools are developed, such as the CO_2 emissions estimator, to assess the impact of our products.

Seals are sustainable by nature, as their main function consists of preventing spillage of lubricant into the environment and protecting rotating equipment from external contamination, thereby enabling extension of machine service life. However, to ensure this main function seals also play a significant role in the friction of rotating equipment, accounting for up to 60% of the total friction torque in some applications. Reducing seal friction is a key customer requirement to enhance system efficiency, lower energy consumption, and minimize overall carbon emissions. With stricter CO_2 regulations, designing optimal sealing solutions that balance low friction with effective sealing performance remains a challenge. Accurate prediction of seal transient dynamics and friction, aided by simulation tools, is essential for accelerating product development and achieving customer-defined friction targets.

In lubricated contact conditions, adhesion effects are significantly reduced and friction originates predominantly from two main sources: viscous shearing of the lubricant in the contact and direct asperity contacts (viscoelastic friction). The contribution from these components depends on various parameters, with the lubrication regime being a critical factor. Material friction can be significant in boundary and mixed lubrication regimes when surfaces are not fully separated by a lubricant film. Conversely, in the full-film lubrication regime, lubricant viscous shearing dominates. Sealing applications can experience all these lubrication regimes during operation. Combining the results of dry (material) friction estimated from the proposed model with viscous shearing effects allows us to determine the overall seal friction. Therefore, this new model serves as a valuable tool for optimizing new sealing solutions towards reduced friction. For example, to minimize material friction, different seal materials can be ranked based on the dry friction coefficient estimated virtually within the relevant range of application conditions.

To illustrate such virtual material selection process, Figure 11 shows the estimated dry friction coefficient for three different proprietary NBR (nitrile butadiene rubber) compounds at a nominal contact pressure of 0.2MPa and temperature and speed range of 25 to 60^{0}C and 10 to 100mm/s respectively. Figure 11 and Table 2 clearly show that there can be substantial difference in dry friction depending on the rubber compound. Assuming that all three compounds satisfy other seal design requirements, then choosing NBR2 over NBR1 enables to reduce the contribution of material dry friction by **~55%** on average. However, the overall seal friction will not be reduced by 55% due to the unaccounted lubricant viscous friction contribution. Nevertheless, it can be safely assumed that at least 30% of the overall friction torque will be caused by material dry friction. In that case, selecting the right material leads to a net reduction in overall friction torque by 0.55*0.3**~16.5%**.

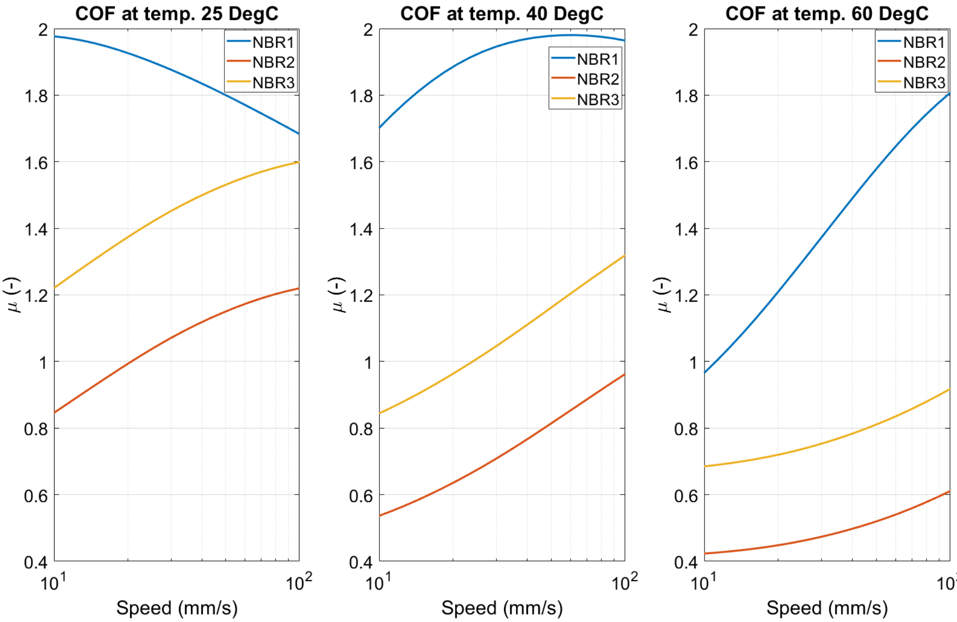

Figure 11: Estimated coefficient of friction (COF) comparison for three different NBR compounds in the temperature and speed range of 25-60°C and 10-100mm/s respectively

Table 2: Estimated COF comparison for different NBR compounds

Material	Average COF (Temperature: 25-60°C Speed: 10-100mm/s)
NBR1	1.72
NBR2	0.76
NBR3	1.09

To demonstrate the potential of sustainable seal design, an example of railway wheel bearing unit system is considered which is gaining an increased attention to reduce friction. Assuming 6 wagons per train, 2 bogies per wagon and 4 bearings per bogie leads to total of 48 bearing units. Each bearing unit has 2 seals and furthermore assuming a realistic reference torque of 0.8Nm per seal based on the test data results in a total seal frictional torque of 1.6Nm per bearing unit system. Therefore the reduced seal frictional torque for optimized seal material (NBR2) is expected to be 1.37Nm per bearing unit (16.5% less). Based on this estimate and using aforementioned SKFs CO2 emissions estimator, the net reduction in CO2 emission using NBR2 sealing material (scenario # 2) over NBR1 sealing material (scenario # 1) for total wheel bearing units (48x) on yearly basis can be estimated as depicted in Figure 12. The CO_2

emissions due to estimated frictional losses are calculated based on the regional CO_2 emissions per kWh for the chosen geographical location. In this example, the chosen region is European union for which the CO_2 conversion factors are used from the Greenhouse Gas Protocol [7].

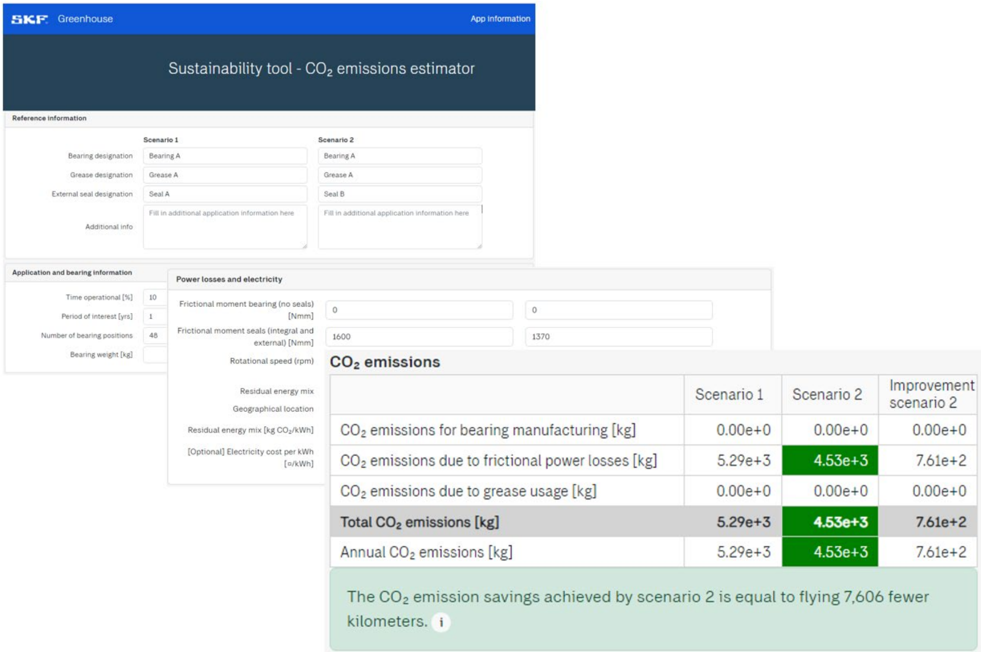

Figure 12: CO_2 emission - estimation using SKFs CO_2 estimator

5 Summary and conclusions

Rubber friction is a complex phenomenon, which is fundamentally related to the viscoelastic nature of the material in question and the multi-scale character of the counterface. Three physical phenomena are involved in rubber friction: lubricant shearing, viscoelastic losses due to the deformation of rubber by the counterface roughness and intermolecular interactions (adhesion) between the two surfaces. In this paper, an enhanced 1st order approach based on viscoelastic energy dissipation at different counterface roughness scales has been developed. This approach allows for rapid prediction of rubber dry friction. The method is applicable for seals and can be coupled with friction due to lubricant viscous shearing to estimate the overall seal friction. The model does not yet take into account the adhesion contribution, although the fitting parameter k_f indirectly accounts for its effect.

The predictions emphasize the importance of the multi-scale surface effects and the relation between rubber material properties and rubber friction under dry condition. Comparison with experiments showed the validity of this approach developed to model rubber dry friction. Finally, this simple yet effective model can be used to compare the dry friction characteristics of different sealing compounds and thereby assisting seal designers in selecting the optimal compound for sustainable and efficient sealing solutions.

6 References

[1] K. A. Grosch, "The Relation Between the Friction and Visco-Elastic Properties of Rubber," *Proc. R. Soc. London, Ser. A, 274,* p. 21–39, 1963.

[2] M. L. Williams, R. F. Landel and J. D. Ferry, "The temperature dependence of relaxation mechanisms in amorphous polymers and other glass-forming liquids.," *Journal of the American Chemical society 77, no. 14,* pp. 3701-3707, 1955.

[3] M. Klüppel and G. Heinrich, *Rubber Chem. Technol.,* pp. 73,578–606, 2000.

[4] B. Persson, "Theory of rubber friction and contact mechanics," *J. Chem. Phys.,* pp. 115, 3840–3861, 2001.

[5] D. B. Wassink, V. G. Lenss, J. A. Levitt and K. C. Ludema, "Physically Based Modeling of Reciprocating Lip Seal Friction," *J. Trib., 123(2),* pp. 404-412, 2001.

[6] K. L. Johnson, Contact mechanics, Cambridge university press., 1987.

[7] "Greenhouse gas protocol," [Online]. Available: https://ghgprotocol.org/tools-resources.

7 Authors

SKF Seals Global Research & Innovation

Meidoornkade 14, 3992 AE Houten, The Netherlands

Dr. Meghshyam Shisode, meghshyam.shisode@skf.com

Dr. Ron Willems, ron.willems@skf.com

Dr. Bas van der Vorst, bas.van.der.vorst@skf.com

Dr. Mickael Sansalone, mickael.sansalone@skf.com

https://doi.org/10.61319/UQVN37SQ